MicroRNA-1236-3p inhibits human osteosarcoma growth

JIARUI LI[1*], JUNXIN CHEN[2*], ZHIJUN HU[2] and WENBIN XU[2]

[1]Department of Urology Surgery, The First Affiliated Hospital of Nanchang University, Medical College of Nanchang University, Nanchang, Jiangxi 330000; [2]Department of Orthopedic Surgery, Sir Run Run Shaw Hospital, Medical College of Zhejiang University & Key Laboratory of Musculoskeletal System Degeneration and Regeneration Translational Research of Zhejiang Province, Hangzhou, Zhejiang 310016, P.R. China

Received February 7, 2020; Accepted September 18, 2020

DOI: 10.3892/ol.2020.12229

Abstract. Osteosarcoma (OS) is a common bone tumor with high mortality worldwide. The long-term survival rate of patients with metastatic or recurrent disease is <20%. The present study explored the biological role of microRNA (miRNA/miR)-1236-3p in OS. miRNA and mRNA expression levels were measured via reverse transcription-quantitative PCR. Fluorescence *in situ* hybridization was performed to determine miR-1236-3p expression levels in clinical specimens. Protein expression was measured via western blotting. Immunohistochemical analysis was used to detect Wnt target gene expression in tumor tissues. The interaction between the Wnt3a 3'untranslated region and miR-1236-3p was assessed via dual-luciferase reporter assays. Cell cycle, Transwell, Cell Counting Kit-8 and wound healing assays were conducted to evaluate the function of the miR-1236-3p/Wnt3a axis. Human OS (HOS) cells stably transfected with vector or miR-1236-3p sponge were injected subcutaneously into nude mice to assess the role of miR-1236-3p *in vivo*. miR-1236-3p expression was downregulated in OS tissues compared with chondroma tissues, and miR-1236-3p overexpression inhibited OS cell migration and proliferation compared with the negative control group. Furthermore, *in vivo* xenograft assays displayed enhanced tumour growth rates in the miR-1236-3p sponge group compared with the vector control group. In the present study, the results indicated that miR-1236-3p inhibited OS progression and Wnt3a was identified as a target of miR-1236-3p.

Correspondence to: Dr Wenbin Xu or Dr Zhijun Hu, Department of Orthopedic Surgery, Sir Run Run Shaw Hospital, Medical College of Zhejiang University & Key Laboratory of Musculoskeletal System Degeneration and Regeneration Translational Research of Zhejiang Province, 3 East Qingchun Road, Hangzhou, Zhejiang 310016, P.R. China
E-mail: xuwenbin@zju.edu.cn
E-mail: hzjspine@zju.edu.cn

Abbreviations: EMT, epithelial-mesenchymal transition; FISH, fluorescence *in situ* hybridization; IHC, immunohistochemical analysis; miRNA/miR, microRNA; NC, negative control; OS, osteosarcoma; UTR, untranslated region

*Contributed equally

Key words: osteosarcoma, miR-1236-3p, Wnt3a, Wnt/β-catenin signaling pathway, epithelial-mesenchymal transformation

Introduction

Osteosarcoma (OS) is the most common bone tumor in children, adolescents and young adults worldwide; its incidence rate among adolescents (15-19 years old) is as high as 8-11 million per year, and the long-term survival rate of metastatic or recurrent patients is <20% (1-3). Previous epidemiological studies of OS revealed a higher prevalence in males, with a peak at 15 years of age (4). Although treatment has improved, its efficacy in patients with metastatic and recurrent OS remains poor (1). Therefore, the identification of new biomarkers and targeted anticancer therapy for OS are required. MicroRNAs (miRNAs/miRs) are endogenous RNAs with ~22 nucleotides (5) that pair with specific bases, such as 3'-untranslated regions (UTRs), to induce RNA degradation or translation inhibition, thereby regulating differentiation, proliferation, apoptosis and other biological processes (6,7).

miR-1236-3p is located within Chr6p21.33 and is embedded within the intron of negative elongation factor E (8). Previous studies have reported that aberrant miR-1236-3p expression is involved in the tumor progression of various types of human cancer, including hepatocellular carcinoma, ovarian carcinoma and renal cell carcinoma (9-11). Moreover, Poos *et al* (12) reported the importance of miRNAs in OS, demonstrating that downregulation of miR-9-5p, miR-138 and miR-214 promoted OS cell proliferation and migration. However, the significance of miR-1236-3p in OS cells is not completely understood. Therefore, the present study aimed to assess the potential use of miR-1236-3p for the diagnosis and treatment of OS.

Materials and methods

Clinical samples. A total of 20 OS tissue and 20 chondroma tissue samples were obtained from 40 patients (including 24 men and 16 women; n=20 per group). The samples were collected between February 2017 and February 2020 at the Second Affiliated Hospital of Zhejiang University (Hangzhou,

China) and Zhejiang Coastal Police Corps Hospital (Jiaxing, China). The OS tissue samples were obtained from patients before the administration of neoadjuvant chemotherapy. All patients or the legal guardians of patients <18 years old provided written informed consent. The present study was approved by the Ethics Committee of Sir Run Run Shaw Hospital. The present study included 40 patients with an average age of 26.8 years (age range, 11-35 years). All OS and chondroma were present in the bones of the patients' limbs. None of the patients with OS displayed metastasis, and pathologists characterized OS and chondroma biopsy samples to the standards defined by the World Health Organization (13). All biopsied specimens were immediately placed in liquid nitrogen and stored at -80˚C.

Cell lines and culture condition. The human osteoblast cell line hFOB1.19 and six human OS cell lines (HOS, 143B, MG63, U2OS, SJSA-1 and SAOS-2) were obtained from Shanghai FuHeng Biological Technology Co., Ltd. The Venor GeM mycoplasma detection kit (Minerva Biolabs GmbH) was used to confirm that all cell lines were free of mycoplasma. All cells were maintained in DMEM (Gibco; Thermo Fisher Scientific, Inc.) supplemented with 10% FBS (Gibco; Thermo Fisher Scientific, Inc.) at 37˚C with 5% CO_2.

Cell transfection. At 50-60% confluence, HOS and U2OS cells were transfected with miR-1236-3p mimic, negative control (NC) mimic, inhibitor NC, miR-1236-3p inhibitor, Wnt3a-small interfering (si)RNA or NC siRNA (10 nM final concentration; Shanghai GenePharma Co., Ltd.) using Lipofectamine® 3000 transfection reagent (Invitrogen; Thermo Fisher Scientific, Inc.) according to the manufacturer's instructions. Subsequent experiments were performed 48 h after cell transfection.

Fluorescence in situ hybridization (FISH). FAM (488)-labeled, locked nucleic acid miR-1236-3p probes were designed and synthesized by Wuhan Servicebio Technology Co., Ltd. The miR-1236-3p probe signals were detected using a commercial FISH kit (Wuhan Servicebio Technology Co., Ltd.) according to the manufacturer's instructions. The images were acquired using an ECLIPSE CI positive fluorescence microscope (Nikon Corporation). Details of the FISH experiment are presented in Data S1.

RNA extraction and reverse transcription-quantitative PCR (RT-qPCR). Total RNA was extracted from OS cells using TRIzol Reagent (CoWin Biosciences) according to the manufacturer's instructions. Total RNA was reverse transcribed into cDNA using the HiFiScipt cDNA Synthesis kit (CoWin Biosciences) at 85˚C for 15 min and 42˚C for 5 min. Subsequently, human miR-1236-3p, Wnt10a, lymphoid enhancer-binding factor 1 (LEF1), Wnt3a, β-catenin, c-Myc and cyclin D1 were amplified via qPCR using the following primers: miR-1236-3p forward, 5'-CCTCTTCCCCTTGTC TCTCCAG-3' and reverse, 5'-TATGGTTGTTCACGACTC CTTCAC-3'; Wnt10a forward, 5'-TGCTCCTGTTCTTCC TACTGC-3' and reverse, 5'-GGGGATCTTGTTGCGAGT CT-3'; LEF1 forward, 5'-TGCATCAGGTACAGGTCCAAG-3' and reverse, 5'-ACGTTGGGAATGAGCTTCGT-3'; Wnt3a forward, 5'-AGTTTGGTGGGATGGTGTCTC-3' and reverse, 5'-CTTGAGGTGCATGTGGCTGG-3'; c-Myc forward, 5'-TCCTCGGATTCTCTGCTC-3' and reverse, 5'-GCTGCG TAGTTGTGCTGATG-3'; and cyclin D1 forward, 5'-TGACCC CGCACGATTTCATT-3' and reverse, 5'-CATGGAGGGCGG ATTGGAAA-3'. qPCR was performed using SYBR® Premix Ex Taq (Takara Bio, Inc.) with StepOnePlus™ Real-Time PCR System (Applied Biosystems; Thermo Fisher Scientific, Inc.) according to the manufacturer's instructions. The following thermocycling conditions were used for qPCR: Initial denaturation at 95˚C for 5 min; followed by 40 cycles of denaturation at 95˚C for 10 sec, annealing at 60˚C for 10 sec and extension at 72˚C for 20 sec. GAPDH and U6 were used as endogenous controls using the following primers: GAPDH forward, 5'-AGC CACATCGCTCAGACAC-3' and reverse, 5'-GCCCAATAC GACCAAATCC-3'; and U6 forward, 5'-AGGGCTGTCTCT GGGAGAAT-3' and reverse, 5'-CTCATGGTTGTGGCTCCC TT-3'. miRNA and mRNA expression levels were calculated using the $2^{-\Delta\Delta Cq}$ method (14).

Cell function experiments. For the colony formation assays, following transfection, cells were seeded into 6-well plates ($1x10^3$ cells/well) and cultured for 10 days without disturbance. The colonies were then fixed with 4% paraformaldehyde for 15 min and stained with 1% crystal violet (Sigma-Aldrich; Merck KGaA) for 30 min at room temperature. A colony was defined as >50 cells and the average number of colonies in 3 separate wells (each group contained 3 wells) was calculated using ImageJ (v2.1.4.7; National Institutes of Health) to assess the colony formation ability.

For the Cell Counting Kit-8 (CCK-8) assays, transfected cells were seeded into 96-well plates ($1x10^3$ cells/well). Cell proliferation ability was determined using CCK-8 reagent (Sigma-Aldrich; Merck KGaA) according to the manufacturer's protocol. Briefly, cell proliferation was measured at 0, 24, 48 and 72 h post-transfection. Cells were incubated with 10 μl/well of CCK-8 solution at 37˚C during the last 1 h of the culture. A microplate reader was then used to detect the absorbance of each well at 0, 24, 48 and 72 h (wavelength, 450 nm).

A Transwell migration assay was conducted to assess OS cell migration. The Transwell system was a 24-well Boyden chamber with a polycarbonate membrane (pore size, 8 mm). A total of $5x10^3$ transfected cells suspended in 200 μl serum-free DMEM were plated into the upper chamber. The lower chamber was filled with DMEM supplemented with 10% FBS. The Transwell system was incubated at 37˚C with 5% CO_2. Following incubation for 24 h, migratory cells were fixed with 4% paraformaldehyde for 15 min and stained with 0.5% crystal violet for 30 min at room temperature. Migratory cells were counted by inverted light microscopy in three randomly selected fields of view and analyzed (magnification, x100).

For the wound healing assay, transfected cells were starved using serum-free medium for 24 h and then seeded into 6-well plates and cultured in serum-free DMEM. At 90-100% confluence, a linear scratch was created using a 200 μl pipette tip and cells were washed three times with PBS. An inverted light microscope was used to visualize the wounds at 0 and 24 h (magnification, x40). All the aforementioned cell function experiments were performed three times.

Flow cytometry for cell cycle analysis. HOS and U2OS cells were starved using serum-free medium for 24 h prior to transfection with miR-1236-3p mimic or Wnt3a siRNA. At 48 h post-transfection, $2x10^6$ cells were fixed with 75% ice-cold ethanol overnight. Subsequently, cells were stained with PI working solution for 15 min at room temperature using the Annexin V-FITC/PI Apoptosis Detection kit (BD Biosciences) according to the manufacturer's protocol. Data were collected on BD FACSCanto (BD Biosciences) and analyzed using FlowJo 10 software (FlowJo LLC). The assay was performed three times.

Protein extraction and western blotting. Total protein was extracted from cells using radioimmunoprecipitation assay lysis buffer (EMD Millipore) and the protein concentration was quantified using a bicinchoninic acid protein assay kit (EMD Millipore). The same amount of protein (30 μg/lane) was separated via 5-10% SDS-PAGE and transferred to PVDF membranes (EMD Millipore) using a semi-dry blotting apparatus (Bio-Rad Laboratories, Inc.). The membranes were blocked with 5% (w/v) non-fat milk in Tris-buffered saline with Tween-20 (100 mM NaCl, 50 mM Tris and 0.1% Tween-20) at room temperature for 1 h. The membranes were incubated at 4˚C overnight with the following primary antibodies: Anti-Wnt3a (cat. no. 2391; 1:1,000; Cell Signaling Technology, Inc.), anti-β-catenin (cat. no. 51067-2-AP; 1:5,000), anti-cyclin D1 (cat. no. 60186-1-lg; 1:1,000;), anti-c-Myc (cat. no. 10828-1-AP; 1:2,000), anti-vimentin (cat. no. 10366-1-AP; 1:2,000), anti-N-cadherin (cat. no. 22018-1-AP; 1:2,000) and anti-GAPDH (cat. no. 10494-1-AP; 1:2,000) (purchased from ProteinTech Group, Inc.). Following primary antibody incubation, the membranes were incubated with HRP-conjugated secondary antibodies (cat. no. SA00001-1 and SA00001-2; 1:5,000; ProteinTech Group, Inc.) for 1 h at 37˚C. ECL Luminous Liquid (EMD Millipore) was used to visualize the bands. GAPDH expression was used as the internal control.

miR-1236-3p target gene prediction and pathway enrichment analysis. TargetScan (version 3.1; http://www.targetscan.org/mamm_31/) and miRanda (http://www.microrna.org/microrna/home.do) were used to predict the target genes of miR-1236-3p. Venny (version 2.1.0; http://bioinfogp.cnb.csic.es/tools/venny/index.html) was used to screen overlapping target genes between TargetScan and miRanda. The Database for Annotation, Visualization and Integrated Discovery (https://david.ncifcrf.gov/) was then used to perform Kyoto Encyclopedia of Genes and Genomes (KEGG) pathway enrichment analyses for the overlapping target genes. KEGG was used to predict the main pathways affected by miR-1236-3p. $P<0.05$ was considered as the cut-off value.

Dual luciferase reporter assay. The putative target genes of miR-1236-3p were predicted using TargetScan. Firefly luciferase (FL) and *Renilla* luciferase (RL) reporter vectors were synthesized by Shanghai GeneChem Co., Ltd. 293T cells (Shanghai FuHeng Biological Technology Co., Ltd.) were seeded into 96-well plates and grown to 30% confluence 24 h before transfection. Subsequently, miR-1236-3p mimic or NC mimic (10 nM final concentration) was co-transfected with 50 ng RL reporter vector and 5 ng FL reporter vector with or without the Wnt3a 3'-UTR using Lipofectamine 3000. At 48 h post-transfection, the Dual-Luciferase Reporter Assay System (Promega Corporation) was used to measure firefly and *Renilla* luciferase activities according to the manufacturer's instructions. The assays were performed three times.

Immunohistochemical (IHC) analysis. Paraffin-embedded samples were dewaxed with xylene and rehydrated with graded ethanol. The samples were incubated overnight at 4˚C with the following primary antibodies (all 1:100; ProteinTech Group, Inc.): Anti-β-catenin (cat. no. 51067-2-AP), c-Myc (cat. no. 10828-1-AP), cyclin D1 (cat. no. 60186-1-lg), Wnt3a (cat. no. HZ-1296) and vimentin (cat. no. 10366-1-AP). Following primary incubation, samples were incubated with universal secondary antibodies (HRP-labeled). Finally, the positive detection rate was used to score the IHC results and staining intensity. Further details of the IHC analysis are presented in Data S1.

Tumor xenograft model in nude mice. The miR-1236-3p sponge, empty vector and packing plasmids (pSPAX2 and pMD2G) were obtained from Shanghai GeneChem Co., Ltd. Packaging plasmids (1.5 μg pSPAX2 and 0.5 μg pMD2G) were co-transfected with 2 μg viral vectors (miR-1236-3p sponge or empty vector) into $7x10^6$ 293T cells. At 24 h post-transfection, the transfected 293T cell medium was used to infect HOS cells according to the manufacturer's protocol. After 48 h, 1 μg/ml puromycin was used to select the infected cells. After 72 h, transfected HOS cells ($4x10^6$) were suspended in 200 μl PBS and, following anesthetization via isoflurane inhalation (3%), they were subcutaneously injected into the junction of the right hindlimb and the hip of nude mice (8 male mice; age, 3-4 weeks; Animal Experimental Center of Sir Run Run Shaw Hospital of Zhejiang University). Control mice were injected with vector-transfected HOS cells and experimental mice were injected with miR-1236-3p sponge-transfected HOS cells. All mice were fed by the animal room staff and monitored every 7 days for the measurement of tumor volume (mm^3; length x width^2 x1/2) (15). After 5 weeks, three nude mice presented tumor ulcers on the site where the tumor cells had been implanted. At this point, the experiment was immediately terminated and the mice were sacrificed via cervical dislocation. After confirming the onset of rigor mortis, the tumors were harvested and weighed. Each group included 4 mice. The humane endpoints established in the present study were as follows: i) Loss of appetite, when nude mice completely lost appetite for 24 h; ii) weakness, unable to eat and drink by themselves, unable to stand for up to 24 h or extremely reluctant to stand; iii) tumor, the tumor volume was >1,500 mm^3, the tumor metastasized or the tumor grew rapidly to ulceration, causing infection or necrosis; iv) musculoskeletal system, muscle damage, bone damage and limbs unable to move; v) nervous system, abnormal central nervous response (twitching, trembling, paralysis and crooked head); and vi) death, when the animal was mentally depressed without hypoesthesia or sedation, accompanied by hypothermia (<37˚C).

Statistical analysis. Statistical analyses were performed using GraphPad Prism software (version 5; GraphPad Software,

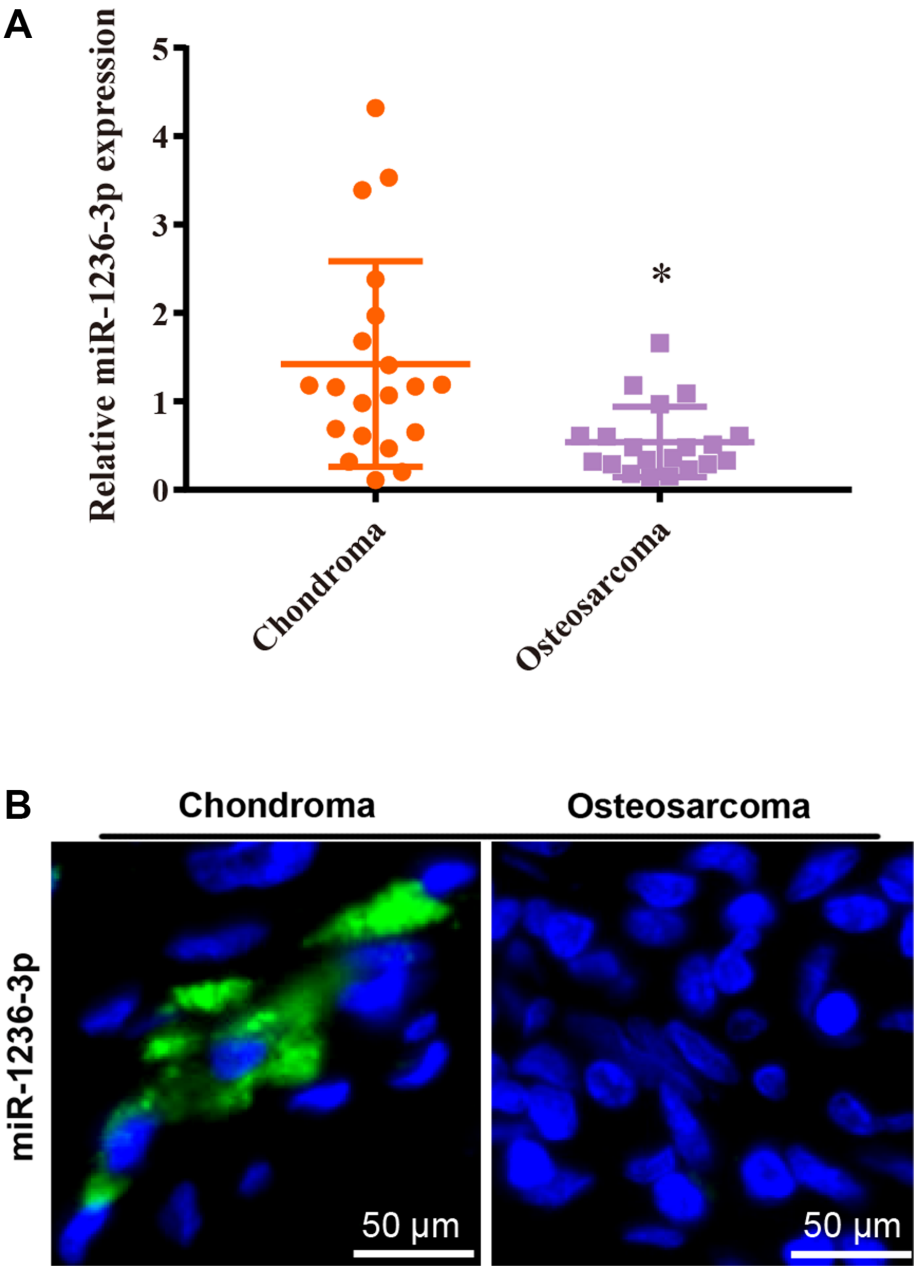

Figure 1. miR-1236-3p expression in OS tissues and cell lines. (A) miR-1236-3p expression levels in OS tissues (n=20) and chondroma tissues (n=20) were measured via reverse transcription-quantitative PCR. *P<0.05 vs. chondroma. (B) miR-1236-3p expression levels in OS and chondroma tissues were measured via fluorescence *in situ* hybridization (scale bar, 50 μm). miR, microRNA; OS, osteosarcoma.

Inc.). Data are presented as the mean ± SD (n=3). The unpaired Student's t-test was used to analyze comparisons between groups. P<0.05 was considered to indicate a statistically significant difference.

Results

Reduced miR-1236-3p in OS tissues and cell lines. The RT-qPCR results indicated that miR-1236-3p expression levels were significantly decreased in OS tissues compared with chondroma tissues (Fig. 1A), which was consistent with the FISH assay results (Fig. 1B).

miR-1236-3p inhibits HOS and U2OS cell proliferation and migration. Aberrant miR-1236-3p expression prompted further investigation of its role in OS. miR-1236-3p mimic was transfected into HOS and U2OS OS cell lines to investigate the function of miR-1236-3p in OS. The RT-qPCR results suggested that miR-1236-3p mimic significantly increased miR-1236-3p expression in HOS and U2OS cells compared with NC mimic (Fig. 2A). The CCK-8 and colony formation assays were conducted to evaluate HOS and U2OS cell proliferation following transfection with miR-1236-3p mimic (Fig. 2B and C). The results indicated an inhibitory role of miR-1236-3p in OS cell proliferation, as demonstrated by significantly decreased cell proliferation and colony formation in the miR-1236-3p mimic group compared with the NC mimic group. As shown in Fig. 2D and E, miR-1236-3p mimic significantly inhibited HOS and U2OS cell migration compared with NC mimic.

The flow cytometry results also suggested that miR-1236-3p overexpression arrested the cell cycle at the G_1 phase in both cell lines (Fig. 2F).

Wnt3a is the target of miR-1236-3p in OS cells and miR-1236-3p inhibits Wnt3a expression. miR-1236-3p overexpression significantly decreased OS cell migration and proliferation and blocked the cell cycle, prompting the exploration of the target genes associated with the regulation of OS cell progression. TargetScan and miRanda were used to predict 5,728 and 3,206 miR-1236-3p target genes, respectively, with 2,218 overlapping genes (Fig. 3A). By conducting pathway enrichment analysis, 'pathways in cancer' was identified as the most likely pathway targeted by miR-1236-3p (Fig. 3B). Numerous literature reports on the role of the Wnt signaling pathway in osteosarcoma have been published (16-18); therefore, the genes in the signaling Wnt pathway (Wnt3a, Wnt10a and LEF1) were selected for further investigation. Compared with NC mimic, miR-1236-3p overexpression significantly decreased LEF1, Wnt3a and Wnt10a expression levels, with Wnt3a expression levels being decreased to the lowest levels among the three genes (Fig. 3C). The base pairing between the 3'UTR of Wnt3a and miR-1236-3p was predicted using TargetScan (Fig. 3D). To test the targeting effect of miR-1236-3p on Wnt3a, dual luciferase reporter assays were performed to assess the association between miR-1236-3p and the potential binding site. Compared with NC mimic, miR-1236-3p overexpression significantly decreased the relative luciferase activity of Wnt3a (Fig. 3E). Western blotting and RT-qPCR were performed to determine the expression of Wnt3a and its downstream genes in HOS and U2OS cells. The downstream genes of Wnt3a include c-Myc, cyclin D1, β-catenin, N-cadherin and vimentin (15). c-Myc and cyclin D1 are closely related to cell cycle regulation, whereas N-cadherin and vimentin are key molecular markers of epithelial-mesenchymal transition (EMT) (19,20). As presented in Fig. 3F and G, miR-1236-3p overexpression decreased the expression levels of Wnt3a and its downstream genes compared with the NC mimic group. In addition, the RT-qPCR results suggested that miR-1236-3p inhibitor significantly downregulated miR-1236-3p expression compared with inhibitor NC (Fig. 3H), which significantly increased the expression of Wnt3a and its downstream genes, including cyclin D1 and c-Myc (Fig. 3I).

Wnt3a knockdown decreases OS cell migration and proliferation. Based on the finding that the 3'UTR of Wnt3a contained a binding site for miR-1236-3p, the biological role of Wnt3a in OS cells was explored. The IHC results indicated that Wnt3a, β-catenin and downstream genes (c-Myc and cyclin D1) were upregulated in OS tissues compared with control chondroma tissues (Fig. 4A). The RT-qPCR results also indicated that Wnt3a was significantly upregulated in OS tissues compared with control chondroma tissues (Fig. 4B). Moreover, compared with the control hFOB1.19 cell line, Wnt3a expression levels were significantly increased in the OS cell lines (HOS, U2OS, MG63, 143B, SJSA-1 and SAOS-2; Fig. 4C). Due to the relatively strong proliferation ability of HOS cells and the relatively high level of Wnt3a expression in U2OS cells, HOS and U2OS cells were selected for subsequent experiments. To investigate the role of Wnt3a in OS cell migration and proliferation, OS cells were transfected with Wnt3a-siRNA or NC, followed by cell function experiments. RT-qPCR and western blotting were performed to verify the transfection efficiency of Wnt3a-siRNA (Fig. 4D and E). The CCK-8 and colony formation assays were conducted to evaluate HOS and U2OS cell proliferation following transfection with Wnt3a-siRNA (Fig. 4F and G). The results indicated that Wnt3a knockdown significantly decreased OS cell proliferation compared with NC. In addition, Wnt3a knockdown significantly inhibited HOS and U2OS cell migration compared with NC (Fig. 4H and I). The flow cytometry results suggested that Wnt3a knockdown also arrested the cell cycle at the G_1 phase for both HOS and U2OS cells (Fig. 4J).

miR-1236-3p overexpression decreases OS cell proliferation in vivo. To further investigate the inhibitory effect of miR-1236-3p on OS cell proliferation, nude mice were subcutaneously injected with HOS cells transfected with miR-1236-3p sponge or vector. Tumor growth was faster in the miR-1236-3p sponge group compared with the vector group, with the longest width of the largest tumor being 1.85 (1.00 cm in control group); Fig. 5A-C). In addition, the FISH assay results indicated that miR-1236-3p sponge markedly reduced miR-1236-3p expression in tumor tissues compared with the vector group (Fig. 5D). miR-1236-3p sponge also increased the mean positive area for Wnt3a, β-catenin, vimentin, c-Myc and cyclin D1 in tumor tissues compared with the vector group, as determined via IHC analysis (Fig. 5E). Detailed records of the tumor sizes throughout the experience are presented in Table SI.

Discussion

OS is a common malignant orthopedic tumor (3). Neoadjuvant chemotherapy with intercalated surgery is an effective treatment strategy for patients with resectable OS who are aged <40 years. However, the prognosis is often poor in patients with metastasis or recurrence, and in patients aged >40 years (21). Low miR-1236-3p expression is associated with gastric cancer (8), ovarian carcinoma (11) and lung adenocarcinoma (22). However, the effect of miR-1236-3p on OS cell invasion and proliferation has not yet been studied.

In the present study, the FISH results indicated markedly lower miR-1236-3p expression levels in OS tissues compared with chondroma tissue. Therefore, to investigate whether low miR-1236-3p expression was related to OS cell proliferation and migration, rescue experiments were performed by transfecting OS cells with miR-1236-3p mimic, which resulted in increased miR-1236-3p expression compared with the NC mimic group. Consequently, the cell function experiment results suggested that miR-1236-3p overexpression significantly decreased OS cell proliferation and migration compared with NC mimic. In addition, the flow cytometry results indicated that miR-1236-3p overexpression inhibited OS cell proliferation by inducing cell cycle arrest at the G_1 phase.

The functional role of the Wnt signaling pathway in OS is not completely understood (23). A number of studies support the idea that the Wnt signaling pathway serves an anti-tumorigenic effect in OS (24-26), whereas other studies suggest that aberrant

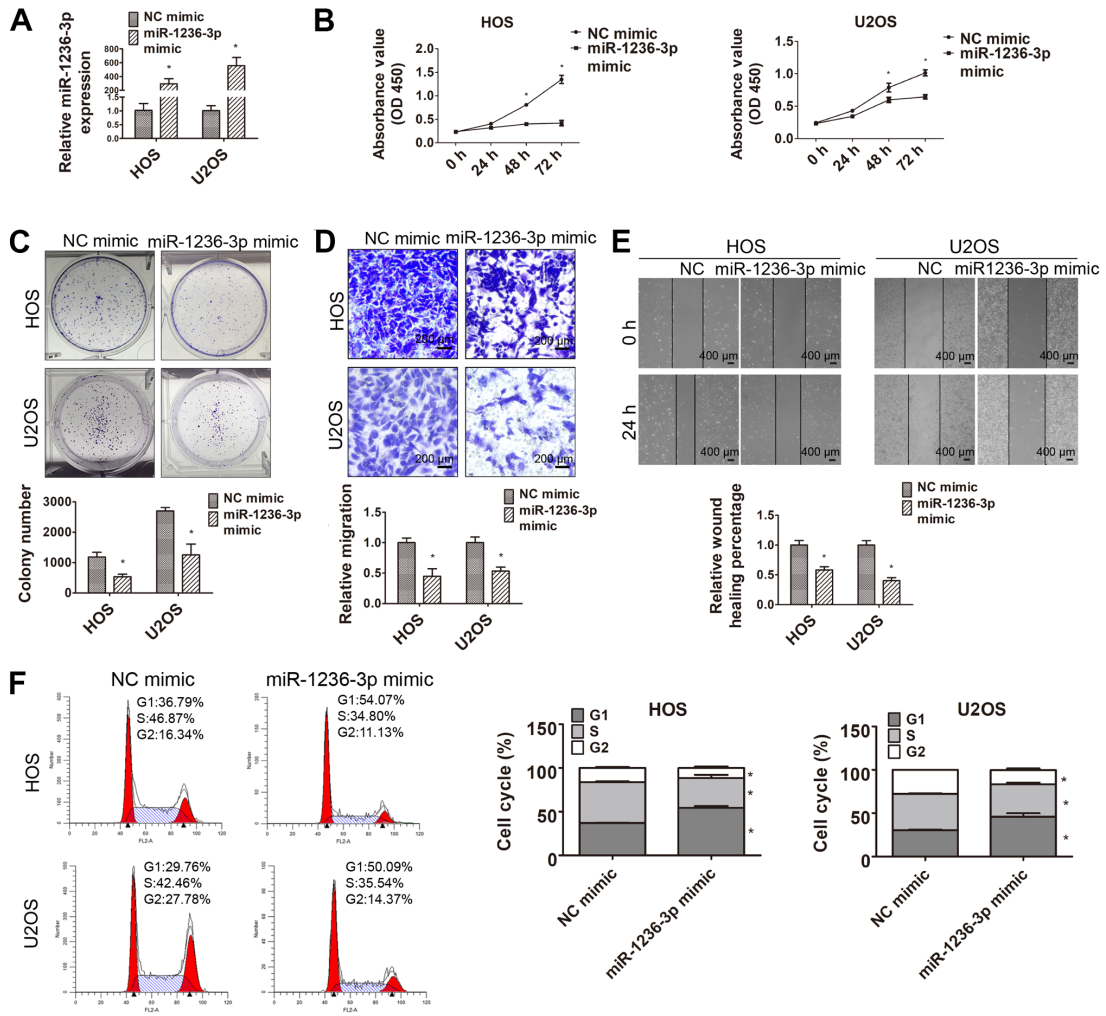

Figure 2. miR-1236-3p overexpression-mediated alterations in OS cells. (A) Relative miR-1236-3p expression levels in HOS and U2OS cell lines following transfection with NC mimic or miR-1236-3p mimic. (B) The Cell Counting Kit-8 assay was performed to assess cell proliferation following transfection with NC mimic or miR-1236-3p mimic at 0, 24, 48 and 72 h. (C) Relative long-term cell proliferation was evaluated by performing the colony formation assay following transfection with NC mimic or miR-1236-3p mimic. (D) The Transwell migration assay was conducted to evaluate HOS and U2OS cell migration following transfection with NC mimic or miR-1236-3p mimic (scale bar, 200 μm). (E) The effect of miR-1236-3p overexpression on HOS and U2OS cell migration was assessed by performing the wound healing assay (scale bar, 400 μm). (F) The cell cycle distribution in HOS and U2OS cell lines following transfection with miR-1236-3p mimic or NC mimic was analyzed via flow cytometry. *P<0.05 vs. NC mimic. miR, microRNA; OS, osteosarcoma; NC, negative control; OD, optical density.

activation of the canonical Wnt signaling pathway serves an important role in OS initiation, maintenance and resistance to chemotherapy (27,28). In addition, a large number of studies have demonstrated that miRNA has an effect on the development of OS by targeting the Wnt signaling pathway. For example, miR-130b enhanced OS cell proliferation by targeting naked cuticle homology 2, a negative regulator of the Wnt signaling pathway (29,30). Yang *et al* (31) reported that miR-425-5p inhibited tumorigenesis via the Wnt/β-catenin signaling pathway in OS. The canonical Wnt pathway is initiated by the binding of appropriate Wnt ligands to the Frizzled and low-density lipoprotein receptor-related protein 5/6 co-receptor. Under normal conditions, without proper Wnt ligands (Wnt-1, Wnt-2, Wnt-3, Wnt-3a, Wnt-4, Wnt-8 and Wnt-10b), excess β-catenin in the cytoplasm is degraded by a multi-protein complex comprised of glycogen synthase kinase 3β, adenomatous polyposis coli and axin (32). When the Wnt signaling pathway is activated, β-catenin can no longer be degraded, and instead it accumulates in the cytosol and enters the nucleus to form a transcriptional complex with the T-cell factor/lymphoid enhancer-binding factor family, activating the expression of a wide range of downstream genes, including c-Myc, cyclin D1, vimentin and N-cadherin (32-34). c-Myc and cyclin D1 are cell cycle-related proteins that can induce cell cycle arrest at the G_1 phase (19). In addition, EMT is closely associated with the migratory ability of tumor cells and oncogenic EMT has been reported to upregulate vimentin and N-cadherin expression levels (20).

Compared with the human osteoblast cell line (hFOB1.19), the expression of Wnt3a was significantly increased in OS cell lines. Furthermore, the base pairing between the 3'UTR of Wnt3a and miR-1236-3p was identified, and miR-1236-3p overexpression inhibited Wnt3a expression compared with NC mimic, as indicated by the dual luciferase reporter assay results. Subsequently, the results indicated that miR-1236-3p overexpression and knockdown decreased and increased the expression levels of Wnt3a and its downstream genes, respectively, compared with the corresponding NC groups. In conclusion, it was hypothesized that miR-1236-3p regulated

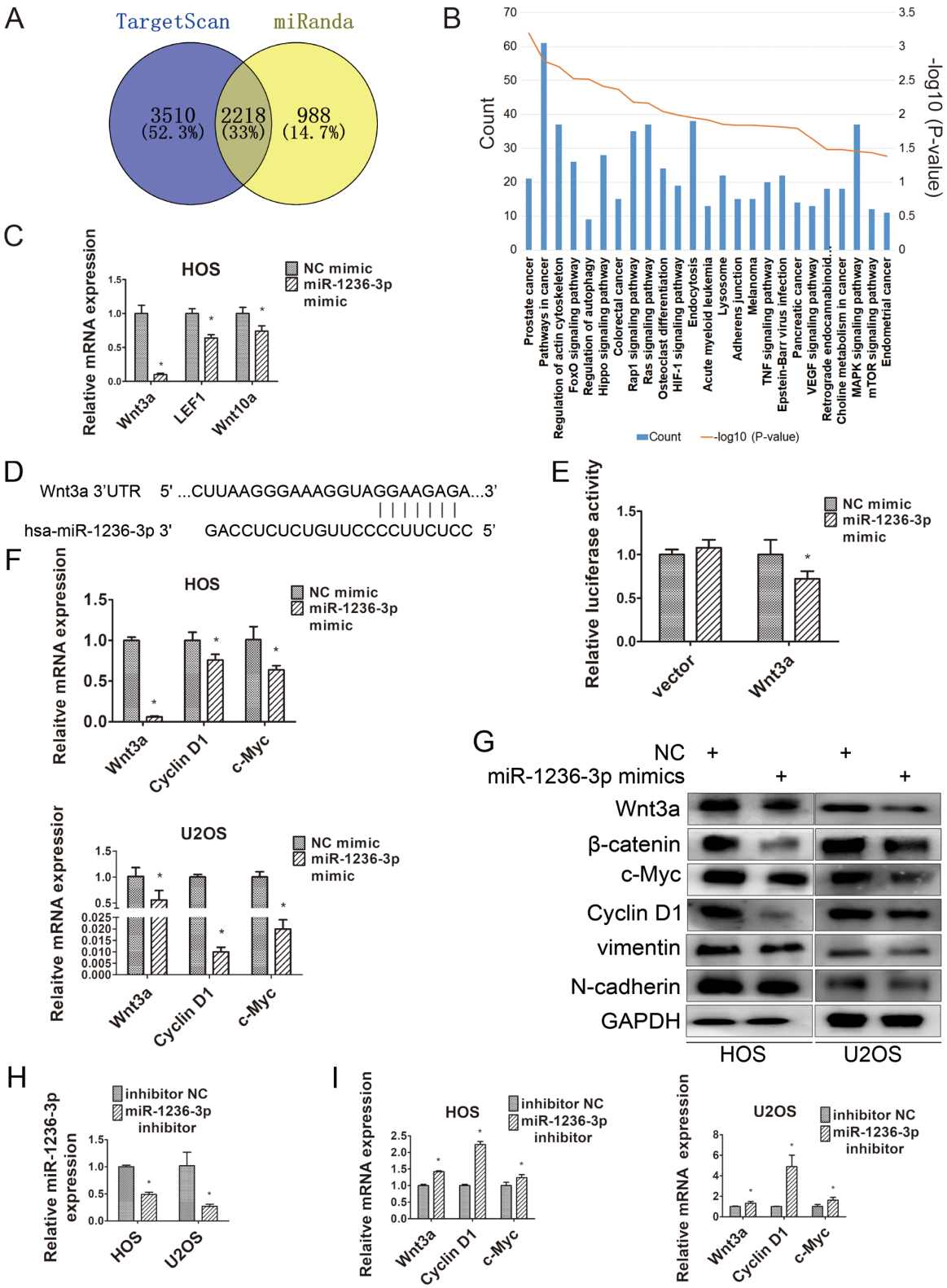

Figure 3. miR-1236-3p affects the Wnt signaling pathway by regulating Wnt3a expression in osteosarcoma cells. (A) The overlapping miR-1236-3p predicted target genes between TargetScan and miRanda. (B) Kyoto Encyclopedia of Genes and Genomes pathways of overlapping genes. (C) miR-1236-3p overexpression significantly decreased Wnt3a, LEF1 and Wnt10a expression levels in HOS cells compared with NC mimic. (D) Base pairing between Wnt3a and miR-1236-3p were predicted using TargetScan. (E) Luciferase Wnt3a 3'UTR reporter or vector constructs were co-transfected into 293T cells with miR-1236-3p mimic or NC mimic. miR-1236-3p overexpression reduced Wnt3a expression and its downstream (F) mRNA and (G) protein levels. (H) Relative miR-1236-3p expression levels in HOS and U2OS cells following transfection with inhibitor NC or miR-1236-3p inhibitor. (I) miR-1236-3p knockdown increased Wnt3a expression and its downstream mRNA levels. *P<0.05 vs. NC. miR, microRNA; LEF1, lymphoid enhancer-binding factor 1; NC, negative control; UTR, untranslated region.

the Wnt signaling pathway by acting on Wnt3a, a Wnt protein reported to activate the signaling pathway (32).

To further investigate whether miR-1236-3p affected OS cell proliferation and migration via targeting Wnt3a, OS cells were

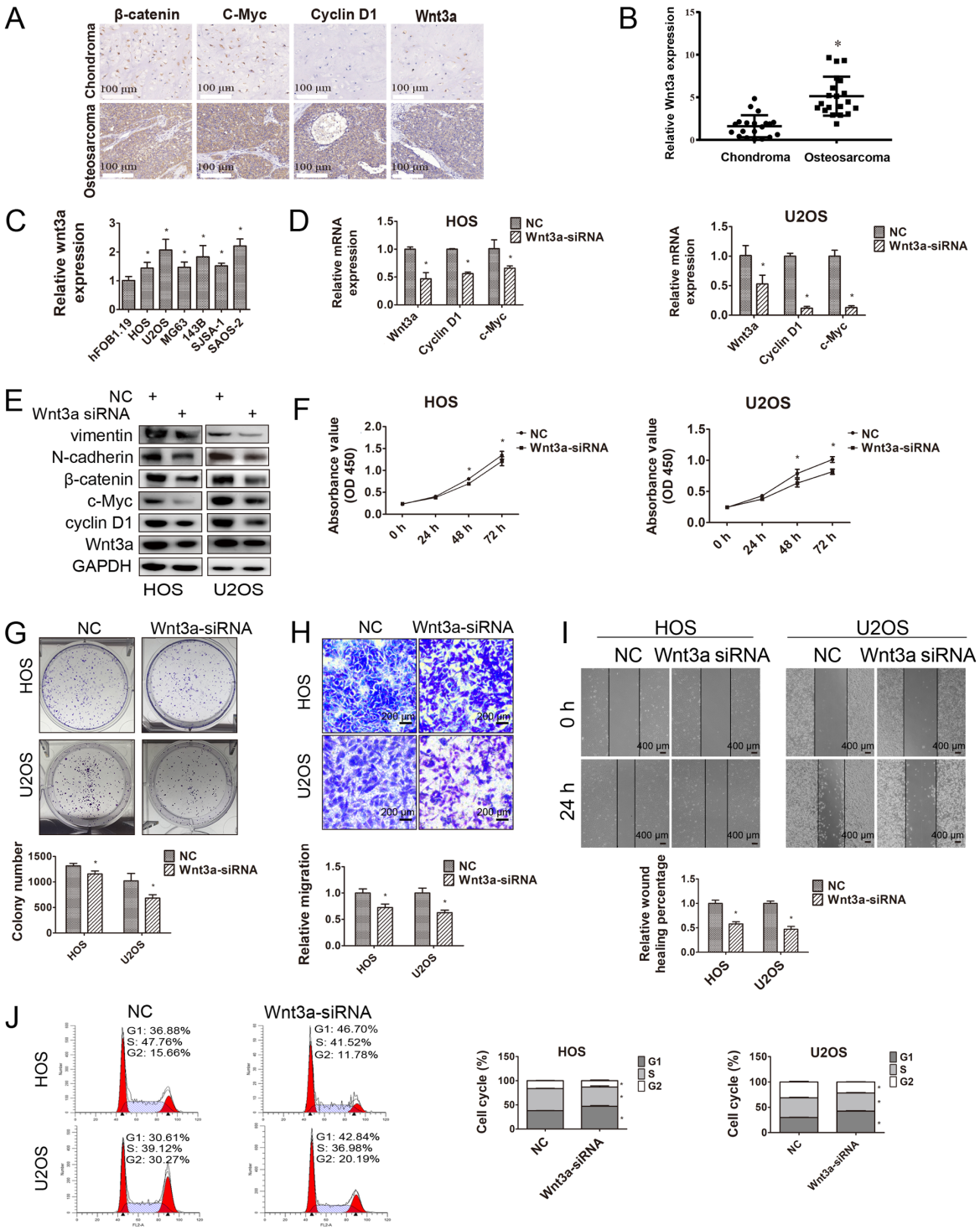

Figure 4. Effects of Wnt3a on OS cells. (A) Wnt3a, β-catenin, c-Myc and cyclin D1 expression levels in OS and chondroma tissues were measured via immunohistochemistry (scale bar, 100 μm). (B) Relative Wnt3a expression in OS tissues (n=20) and chondroma tissues (n=20). *P<0.05 vs. chondroma. (C) Relative Wnt3a expression in hFOB1.19 and OS cell lines (HOS, U2OS, MG63, 143B, SJSA-1 and SAOS-2). Each Student's t-test was evaluated separately for each set of 2 comparisons (hFOB1.19 vs. each of the 6 osteosarcoma cell lines). Wnt3a knockdown decreased the (D) mRNA and (E) protein expression levels of its downstream genes. (F) The Cell Counting Kit-8 assay was performed to assess cell proliferation following transfection with NC or Wnt3a-siRNA at 0, 24, 48 and 72 h. (G) Relative long-term cell proliferation was evaluated by conducting colony formation assays following transfection with NC or Wnt3a-siRNA. (H) Relative HOS and U2OS cell migration was evaluated by performing Transwell migration assays following transfection with NC or Wnt3a-siRNA (scale bar, 200 μm). (I) The effect of Wnt3a on HOS and U2OS cell migration was determined by performing the wound healing assay (scale bar, 400 μm). (J) The cell cycle distribution in HOS and U2OS cell lines following transfection with NC or Wnt3a-siRNA was analyzed via flow cytometry. *P<0.05 vs. NC. OS, osteosarcoma; NC, negative control; siRNA, small interfering RNA; miR, microRNA; OD, optical density.

transfected with Wnt3a-siRNA to downregulate Wnt3a expression. The cell function experiments, cell cycle experiments, RT-qPCR and western blotting results displayed consistent results between Wnt3a knockdown and miR-1236-3p overexpression. The results indicated that miR-1236-3p affected the Wnt signaling pathway by acting on Wnt3a, ultimately affecting

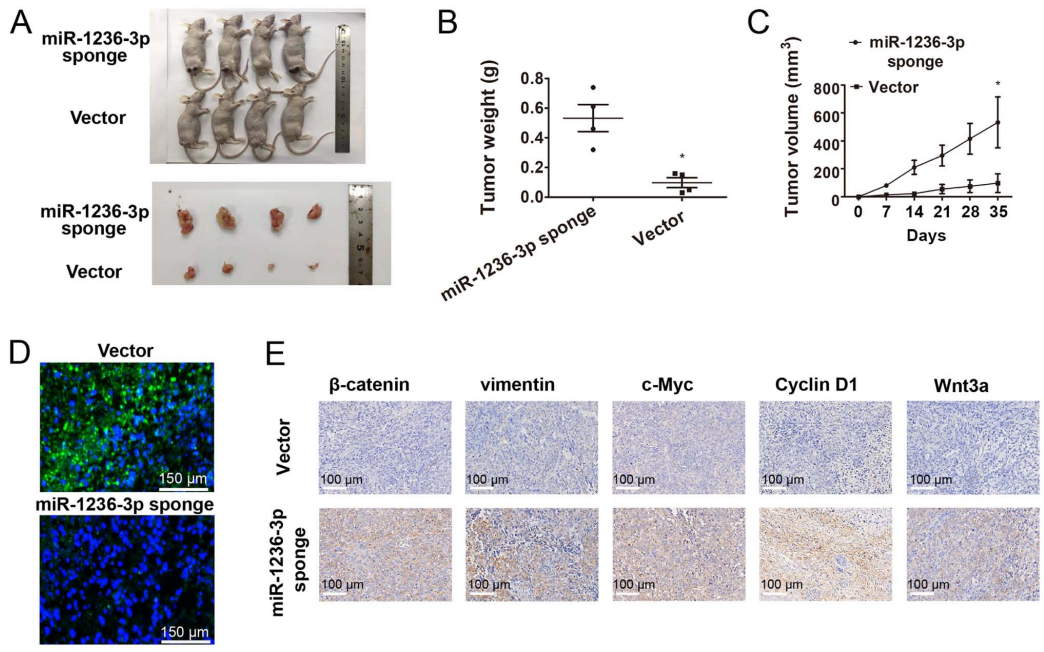

Figure 5. miR-1236-3p inhibits osteosarcoma cell proliferation *in vivo*. (A) Nude mice were subcutaneously injected with $4x10^6$ HOS stable cells. Each group consisted of four mice and all tumors were harvested after 5 weeks. (B) Average tumor weight in each group. (C) Tumor volume was measured every week according to the following formula: Tumor volume=length x width^2 x 1/2. (D) miR-1236-3p expression in tumor tissues was measured via fluorescence *in situ* hybridization (scale bar, 150 μm). (E) Wnt3a, β-catenin, vimentin, c-Myc, and cyclin D1 expression levels in tumor tissues were measured via immunohistochemical analysis (scale bar, 100 μm). *P<0.05 vs. miR-1236-3p sponge. miR, microRNA.

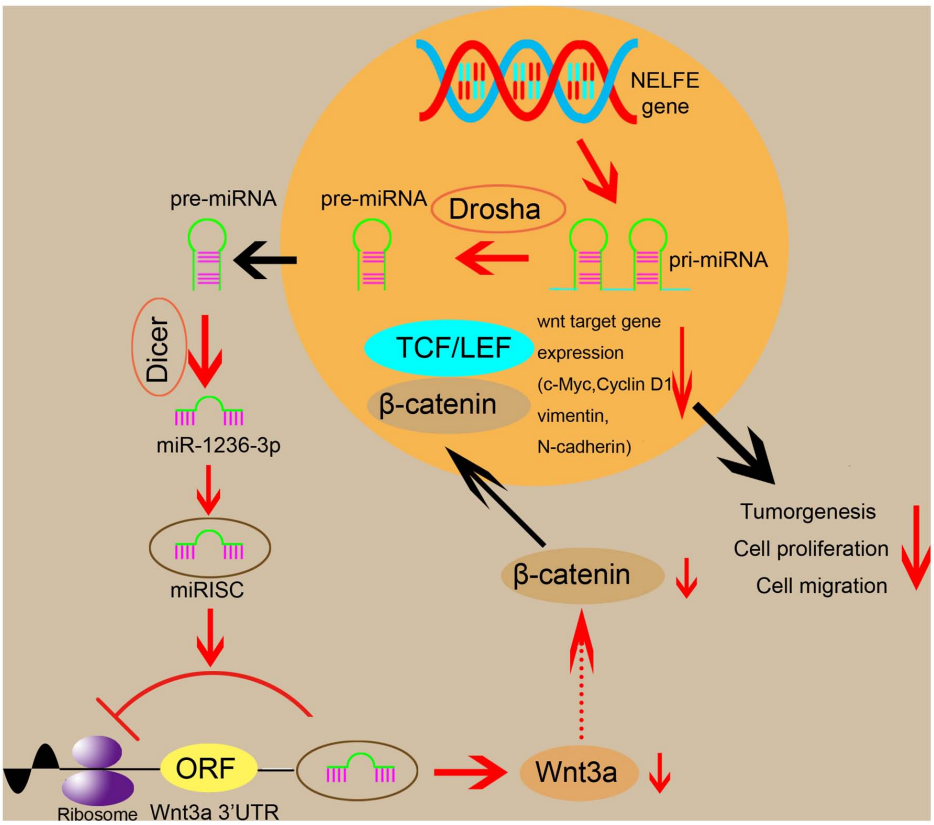

Figure 6. Suggested schematic illustration of the miR-1236-3p/Wnt3a axis in osteosarcoma. miR/miRNA, microRNA; UTR, untranslated region; NELFE, negative elongation factor E; TCF/LEF, T-cell factor/lymphoid enhancer-binding factor; ORF, open reading frame.

OS cell proliferation and migration (Fig. 6). However, the present study had a number of limitations. First, it could not be determined whether miR-1236-3p affected the Wnt signaling pathway via other target genes. Thus, additional studies are

required to assess other links between miR-1236-3p and the Wnt signaling pathway. Second, when constructing the nude mice tumor xenograft models, nude mice were not weighed before and after the experiment, which prevented the analysis of the effect of tumor growth on the body weight of nude mice.

To the best of our knowledge, the present study was the first to explore the relationship between miR-1236-3p and OS. miR-1236-3p inhibited OS cell proliferation and migration by inhibiting the G_1/S transition and EMT. The present study may provide novel insights into the treatment of OS, which may have the potential to be applied in the clinical setting following further investigation.

Acknowledgements

The authors would like to thank Dr Zhe Gong (The Second Affiliated Hospital of Zhejiang University, Hangzhou, China) and Mr Jun Li (Zhejiang Coastal Police Corps Hospital, Jiaxing, China) for their assistance with the experiments.

Funding

The present study was supported by the National Key R&D Program of China (grant no. 2018YFC1105200), the Key Research and Development Plan in Zhejiang Province (grant no. 2018C03060), the National Nature Science Fund of China (grant nos. 81871797, 81874015, 81871796, 81873985, 81802680 and 81802147), the Natural Science Fund of Zhejiang Province (grant nos. Z15H060002, LY16H060004, LY19H160058 and LY16H060002) and the Medical Science and Technology Project of Zhejiang Province of China (grant no. 2017179447).

Availability of data and materials

The datasets used and/or analysed during the current study are available from the corresponding author on reasonable request.

Authors' contributions

WX and ZH designed the present study. JL and JC conducted the experiments and carried out the statistical analysis. JL wrote the paper and WX revised the paper. All authors read and approved the final manuscript.

Ethics approval and consent to participate

All patients provided written informed consent. The present study was approved by the Ethics Committee of Sir Run Run Shaw Hospital. All animal experiments were approved by the Animal Care Committee of Sir Run Run Shaw Hospital.

Patient consent for publication

Not applicable.

Competing interests

The authors declare that they have no competing interests.

References

1. Li Z, Dou P, Liu T and He S: Application of long noncoding RNAs in osteosarcoma: Biomarkers and therapeutic targets. Cell Physiol Biochem 42: 1407-1419, 2017.
2. Isakoff MS, Bielack SS, Meltzer P and Gorlick R: Osteosarcoma: Current treatment and a collaborative pathway to success. J Clin Oncol 33: 3029-3035, 2015.
3. Ritter J and Bielack SS: Osteosarcoma. Ann Oncol 21 (Suppl 7): vii320-vii325, 2010.
4. Stiller CA, Bielack SS, Jundt G and Steliarova-Foucher E: Bone tumours in European children and adolescents, 1978-1997. Report from the automated childhood cancer information system project. Eur J Cancer 42: 2124-2135, 2006.
5. Bartel DP: MicroRNAs: Genomics, biogenesis, mechanism, and function. Cell 116: 281-297, 2004.
6. Kim VN and Nam JW: Genomics of microRNA. Trends Genet 22: 165-173, 2006.
7. Pasquinelli AE, Hunter S and Bracht J: MicroRNAs: A developing story. Curr Opin Genet Dev 15: 200-205, 2005.
8. An JX, Ma MH, Zhang CD, Shao S, Zhou NM and Dai DQ: miR-1236-3p inhibits invasion and metastasis in gastric cancer by targeting MTA2. Cancer Cell Int 18: 66, 2018.
9. Gao R, Cai C, Gan J, Yang X, Shuang Z, Liu M, Li S and Tang H: miR-1236 down-regulates alpha-fetoprotein, thus causing PTEN accumulation, which inhibits the PI3K/Akt pathway and malignant phenotype in hepatoma cells. Oncotarget 6: 6014-6028, 2015.
10. Wang C, Tang K, Li Z, Chen Z, Xu H and Ye Z: Targeted p21(WAF1/CIP1) activation by miR-1236 inhibits cell proliferation and correlates with favorable survival in renal cell carcinoma. Urol Oncol 34: 59.e23-e34, 2016.
11. Wang Y, Yan S, Liu X, Zhang W, Li Y, Dong R, Zhang Q, Yang Q, Yuan C, Shen K and Kong B: miR-1236-3p represses the cell migration and invasion abilities by targeting ZEB1 in high-grade serous ovarian carcinoma. Oncol Rep 31: 1905-1910, 2014.
12. Poos K, Smida J, Nathrath M, Maugg D, Baumhoer D and Korsching E: How microRNA and transcription factor co-regulatory networks affect osteosarcoma cell proliferation. PLoS Comput Biol 9: e1003210, 2013.
13. Jundt G: Updates to the WHO classification of bone tumours. Pathologe 39: 107-116, 2018 (In German).
14. Livak KJ and Schmittgen TD: Analysis of relative gene expression data using real-time quantitative PCR and the 2(-Delta Delta C(T)) method. Methods 25: 402-408, 2001.
15. Chen J, Liu G, Wu Y, Ma J, Wu H, Xie Z, Chen S, Yang Y, Wang S and Shen P, *et al*: CircMYO10 promotes osteosarcoma progression by regulating miR-370-3p/RUVBL1 axis to enhance the transcriptional activity of β-catenin/LEF1 complex via effects on chromatin remodeling. Mol Cancer 18: 150, 2019.
16. Martins-Neves SR, Paiva-Oliveira DI, Fontes-Ribeiro C, Bovée JVMG, Cleton-Jansen A-M and Gomes CMF: IWR-1, a tankyrase inhibitor, attenuates Wnt/β-catenin signaling in cancer stem-like cells and inhibits in vivo the growth of a subcutaneous human osteosarcoma xenograft. Cancer Lett 414: 1-15, 2018.
17. Mu Y, Zhang L, Chen X, Chen S, Shi Y and Li J: Silencing microRNA-27a inhibits proliferation and invasion of human osteosarcoma cells through the SFRP1-dependent Wnt/β-catenin signaling pathway. Biosci Rep 39: BSR20182366, 2019.
18. Li X, Lu Q, Xie W, Wang Y and Wang G: Anti-tumor effects of triptolide on angiogenesis and cell apoptosis in osteosarcoma cells by inducing autophagy via repressing Wnt/β-catenin signaling. Biochem Biophys Res Commun 496: 443-449, 2018.
19. Kaldis P and Pagano M: Wnt signaling in mitosis. Dev Cell 17: 749-750, 2009.
20. Micalizzi DS, Farabaugh SM and Ford HL: Epithelial-mesenchymal transition in cancer: Parallels between normal development and tumor progression. J Mammary Gland Biol Neoplasia 15: 117-134, 2010.
21. Whelan JS and Davis LE: Osteosarcoma, chondrosarcoma, and chordoma. J Clin Oncol 36: 188-193, 2018.
22. Bian T, Jiang D, Liu J, Yuan X, Feng J, Li Q, Zhang Q, Li X, Liu Y and Zhang J: miR-1236-3p suppresses the migration and invasion by targeting KLF8 in lung adenocarcinoma A549 cells. Biochem Biophys Res Commun 492: 461-467, 2017.
23. Zhao SJ, Jiang YQ, Xu NW, Zhang Q, Wang SY, Li J, Wang YH, Zhang YL, Jiang SH, Wang YJ, *et al*: SPARCL1 suppresses osteosarcoma metastasis and recruits macrophages by activation of canonical WNT/β-catenin signaling through stabilization of the WNT-receptor complex. Oncogene 37: 1049-1061, 2018.

24. Matushansky I, Hernando E, Socci ND, Mills JE, Matos TA, Edgar MA, Singer S, Maki RG and Cordon-Cardo C: Derivation of sarcomas from mesenchymal stem cells via inactivation of the Wnt pathway. J Clin Invest 117: 3248-3257, 2007.
25. Cai Y, Mohseny AB, Karperien M, Hogendoorn PC, Zhou G and Cleton-Jansen AM: Inactive Wnt/beta-catenin pathway in conventional high-grade osteosarcoma. J Pathol 220: 24-33, 2010.
26. Basu-Roy U, Seo E, Ramanathapuram L, Rapp TB, Perry JA, Orkin SH, Mansukhani A and Basilico C: Sox2 maintains self renewal of tumor-initiating cells in osteosarcomas. Oncogene 31: 2270-2282, 2012.
27. Pridgeon MG, Grohar PJ, Steensma MR and Williams BO: Wnt signaling in ewing sarcoma, osteosarcoma, and malignant peripheral nerve sheath tumors. Curr Osteoporos Rep 15: 239-246, 2017.
28. Li C, Shi X, Zhou G, Liu X, Wu S and Zhao J: The canonical Wnt-beta-catenin pathway in development and chemotherapy of osteosarcoma. Front Biosci (Landmark Ed) 18: 1384-1391, 2013.
29. Li Z, Li Y, Wang N, Yang L, Zhao W and Zeng X: miR-130b targets NKD2 and regulates the Wnt signaling to promote proliferation and inhibit apoptosis in osteosarcoma cells. Biochem Biophys Res Commun 471: 479-485, 2016.
30. Zhao S, Kurenbekova L, Gao Y, Roos A, Creighton CJ, Rao P, Hicks J, Man TK, Lau C, Brown AM, *et al*: NKD2, a negative regulator of Wnt signaling, suppresses tumor growth and metastasis in osteosarcoma. Oncogene 34: 5069-5079, 2015.
31. Yang G, Zhang C, Wang N and Chen J: miR-425-5p decreases LncRNA MALAT1 and TUG1 expressions and suppresses tumorigenesis in osteosarcoma via Wnt/β-catenin signaling pathway. Int J Biochem Cell Biol 111: 42-51, 2019.
32. Xi Y and Chen Y: Wnt signaling pathway: Implications for therapy in lung cancer and bone metastasis. Cancer Lett 353: 8-16, 2014.
33. Nusse R and Clevers H: Wnt/β-catenin signaling, disease, and emerging therapeutic modalities. Cell 169: 985-999, 2017.
34. Peng Z, Wu T, Li Y, Xu Z, Zhang S, Liu B, Chen Q and Tian D: MicroRNA-370-3p inhibits human glioma cell proliferation and induces cell cycle arrest by directly targeting β-catenin. Brain Res 1644: 53-61, 2016.